

A Proposal for a Parameterized Circulating Vector Field Guidance for Fixed Wing
Unmanned Aerial Vehicles

A thesis presented to
the faculty of
the Russ College of Engineering and Technology of Ohio University

In partial fulfillment
of the requirements for the degree
Master of Science

Garrett S. Clem

May 2018

© 2018 Garrett S. Clem. All Rights Reserved.

This thesis titled

A Proposal for a Parameterized Circulating Vector Field Guidance for Fixed Wing
Unmanned Aerial Vehicles

by

GARRETT S. CLEM

has been approved for

the Department of Mechanical Engineering

and the Russ College of Engineering and Technology by

Jay P. Wilhelm

Assistant Professor of Mechanical Engineering

Dennis Irwin

Dean, Russ College of Engineering and Technology

ABSTRACT

CLEM, GARRETT S., M.S., May 2018, Mechanical Engineering

A Proposal for a Parameterized Circulating Vector Field Guidance for Fixed Wing

Unmanned Aerial Vehicles (47 pp.)

Director of Thesis: Jay P. Wilhelm

Unmanned Aerial Vehicles (UAVs) are guided to fly along straight line obstacle free paths that connect pre-planned waypoints. Initially undiscovered obstacles encountered during flight may require waypoints to be re-planned. Obstacles could be avoided without the need to re-plan mission waypoints by implementing vector field path following in conjunction with repulsive obstacle vector fields. Repulsive vector fields that combine weighted repulsive and attractive components to provide an optimal obstacle avoidance guidance will be investigated to avoid singularities and improve path tracking performance compared to waypoint guidance.

TABLE OF CONTENTS

	Page
Abstract	3
List of Figures	6
List of Symbols	7
List of Acronyms	8
 1 Introduction	9
1.1 Motivation and Problem Statement	9
1.2 Objectives Overview	10
1.3 Phase I	10
1.4 Phase II	10
1.5 Phase III	10
1.6 Summary of Phases	11
 2 Literature Review	13
2.1 Introduction to Literature Review	13
2.2 Unmanned Aerial Vehicle	13
2.3 Path Planning and Guidance	15
2.4 Potential Field	16
2.4.1 Path Following Vector Field Guidance	21
2.5 Vector Field Guidance	21
2.5.1 Introduction to Vector Field Guidance	21
2.5.2 Lyapunov Vector Fields	22
2.5.3 Path Planning Vector Fields	26
2.5.4 Gradient Vector Field	27
2.6 Dubins Vehicle	31
2.7 Unmanned Aerial Vehicle Simulation	32
2.8 Literature Review Summary	32
 3 Methodology	34
3.1 Introduction to Methodology	34
3.2 Phase I	34
3.3 Phase II	40
3.4 Phase III	40

4	Results	41
4.1	Introduction to Results	41
4.2	Phase I	41
4.3	Phase II	41
4.4	Phase III	41
5	Conclusions	42
6	Future Work	43
	References	44

LIST OF FIGURES

Figure	Page
2.1 Fixed wing (a) and multirotor (b) UAVs	13
2.2 Pixhawk autopilot	14
2.3 Autopilot's Navigation, Guidance, and Control Architecture	15
2.4 Single Obstacle Potential Field Gradient [15]	16
2.5 Virtual force field histogram acting on a mobile robot [17]	17
2.6 Potential Field Local Minimum [15]	18
2.7 Potential Field Local Minimum [15]	19
2.8 Obstacle Clustering [15]	19
2.9 UAV avoiding obstacle with VFF Guidance	20
2.10 Lyapunov vector field for straight line and circular primitives [24]	23
2.11 Straight path following in urban environment [24] using Lyapunov Vector Field	24
2.12 Lyapunov vector field approach curved path asymptotically [28]	24
2.13 Elliptical VF produced by non-linear coordinate transformations a) [30] and b) [29]	25
2.14 Tangent plus lyapunov vector fields for shortest path target tracking [32]	26
2.15 RRT* path planner with a VF used as a task specification [34]	27
2.16 Vector field within a set of delaunay triangles [35]	27
2.17 Place holder image of UAV following ground target [2]	30
2.18 Differential drive mobile robot simulating fixed wing UAV Dubins constraints .	32
3.1 Place Intersection	34
3.2 GVF converging and a) small circulation b) large circulation	35
3.3 GVF converging and circulating circular path	35
3.4 GVF circular attractive field without normalization (a) and with normalization (b)	36
3.5 Circular GVF without normalization (a) and with normalization (b)	37
3.6 Circular time-varying GVF without normalization (a) and with normalization (b) .	38
3.7 GVF with unity ($G=H=L=I$) weights for a moving circular path	39

LIST OF SYMBOLS

\vec{v}	Vector field
\vec{v}_{conv}	Convergence component
\vec{v}_{circ}	Circulation component
\vec{v}_{tv}	Time-varying component
G	Convergence weight
H	Circulation weight
L	Time-varying weight
q	Spatial dimension set
$\alpha_i(x_1, x_2, \dots x_n, t)$	Implicit surface function
n	Number of spatial dimensions
t	Time
i	index
∇_q	Gradient with respect to spatial dimensions q
M	Gradient matrix
a	Velocity column vector
\vec{V}	Total field
d	Range
P	Decay weight
R	Radius
$\vec{v}_{repulsive}$	Repulsive vector field
$\vec{v}_{attractive}$	Attractive vector field
u	Speed

LIST OF ACRONYMS

UAV	Unmanned Aerial Vehicles
VF	Vector Field
UAS	Unmanned Aerial System
VFF	Virtual Force Field
TPLVF	Tangent Plus Lyapunov Vector Field
RRT*	Optimal Rapid Radom Trees
DT	Delauny Triangulation
GVF	Gradient Vector Field

1 INTRODUCTION

1.1 Motivation and Problem Statement

Fixed wing Unmanned Aerial Vehicles (UAVs) are used for missions such as surveillance and reconnaissance that might put pilots in harms way [1]. Missions typically consist of sequential objectives represented as waypoints that the UAV follows. Waypoints may be pre-planned before flight where vehicle constraints and obstacles can be considered to prevent collisions or entry into no-fly zones. UAVs follow waypoints by implementing guidance algorithms that calculate headings to direct a UAV along a path connecting the waypoints. Obstacles may be discovered during flight that were unknown at initial planning and a new set of waypoints may have to be generated. Waypoints are typically computed at a ground station and are relayed to the UAV by radio, which may be problematic if communication with the UAV is lost. Guidance that accomplishes mission objectives while avoiding obstacles without the need for re-planning waypoints may be beneficial.

Vector Field (VF) guidance is a method that is mainly used for path following and can be useful for obstacle avoidance [2, 3]. VFs can produce continuous heading vectors that can be used to guide a UAV to coverage and follow a path. Vectors are calculated by summing together convergence and circulation terms that are weighted by static scalars. Obstacles can be represented as a path and given a negative convergence weight resulting in a repulsive field. Static repulsive VFs do not always route the UAV around an obstacle. Modifying repulsive VF parameters to be functions of common UAV states may be used to produce an optimal guidance. **The proposed research seeks to determine VF weighting functions that enable optimal obstacle avoidance.**

1.2 Objectives Overview

The proposed research will be conducted in three phases where VF guidance singularities will be demonstrated, weighting functions will be investigated, and a developed GVF will be validated on a ground robot simulating a UAV. Phases I and II will be conducted in a simulation environment that combines mission paths and obstacles into a single GVF. Phase III will be conducted with a ground robot simulating a UAV guided by the modified GVF in real-time. Dubin's fixed wing constraints will be imposed in simulations and experiments.

1.3 Phase I

Demonstrate GVF singularities for circular obstacles. A simulation environment will be built that generates GVFs consisting of mission paths and obstacles. Circular obstacles will be investigated and the resulting singularities will be characterized. Static weights will be used and the performance of the guidance measured in distance traveled and time of flight.

1.4 Phase II

Investigate GVF weighting functions that influence obstacle avoidance. UAV closing rate, position, and range will be used to develop dynamic GVF weights for convergence and circulation. The modified GVF will be compared against a static and strictly repulsive GVF. Distance traveled and time of flight will be used to as metrics to compare the modified GVF to the unmodified GVF.

1.5 Phase III

Validate modified GVF model with ground robot experiments. The modified GVF developed in Phase II will be implemented on a differential drive ground robot

simulating a fixed wing UAV. Guidance performance while avoiding static obstacles will be demonstrated.

1.6 Summary of Phases

Each phase consists of an **objective** that will be accomplished by executing *tasks*. Completion of all objectives and phases will result in the final deliverable.

Phase I Objective: Demonstrate Gradient Vector Field Singularities

Tasks:

1. *Build a GVF simulation environment*
2. *Evaluate scenarios where singularities are expected*
3. *Characterize location of singularities*

Phase II Objective: Investigate GVF weighting functions that influence obstacle avoidance

Tasks:

1. *Formulate circulation and convergence weights as functions of UAV state*
2. *Determine combination of GVF weights that produces optimal guidance in simulation*

Phase III Objective: Validate modified GVF model with ground robot experiments

Tasks:

1. *Build differential drive robot*
2. *Build robotic framework to take guidance commands*
3. *Repeat simulations performed in Phase II on ground robot*

Deliverable: Adaptive GVF parameterized weights optimal guidance for path following and static obstacle avoidance.

2 LITERATURE REVIEW

2.1 Introduction to Literature Review

2.2 Unmanned Aerial Vehicle

Unmanned Aerial Vehicles (UAVs) are pilotless aircraft used by military, police, and civilian communities for tasks such as reconnaissance, damage assessment, natural disaster surveying, and target tracking [4, 5]. Tasks may be carried out by a single UAV or in cooperation other air or ground vehicles [6–8]. In general, UAVs are categorized into fixed wing and rotor craft varieties [9] that range in size, payload, and flight time capabilities. Fixed wing UAVs (Figure 2.1a) are typically used for tasks that require larger payloads, such as cameras and cargo, and longer flight times. Multirotor UAVs (Figure 2.1b), in general, have lower payload capabilities compared to fixed wing UAVs, however do not require a large clearing for takeoff and landing and have a small turning radius making them more maneuverable.



Figure 2.1: Fixed wing (a) and multirotor (b) UAVs

The aircraft's route can be controlled directly by an operator's radio controller input when the vehicle is within line-of-sight (LOS). For long endurance or beyond LOS missions

the UAV can be guided to navigate a series of waypoints that lie along a pre-planned path by an on-board autopilot such as the Pixhawk, Figure 2.2.



Figure 2.2: Pixhawk autopilot

These UAVs and autopilots are part of an Unmanned Aerial System (UAS) which work in conjunction with ground stations, radio control transmitters, and two way radios. The UAV craft provides the support structure, lifting and control surfaces, and housing for the autopilot, radios, and sensors. Ground stations are responsible for monitoring the vehicle's status, planning missions, and generating obstacle free and flyable paths which are sent to the autopilot via two way radio.

The UAV autopilot is responsible for controlling a pre-planned path and maintaining vehicle stability while under the influence of external wind disturbances. Stable flight while path following is accomplished by implementing feed-back control, navigation, and guidance systems. A high level overview of the autopilots systems can be seen in Figure 2.3. Feed-back refers to the closure of an open-loop control system which allows a reference error to be calculated between the desired state of the UAV, the reference, and the current state of the UAV. Reference error is used to calculate the necessary actuator output required to modify the vehicles attitude and position while preventing unbounded oscillation. Attitude and position feed-back is provided by the navigation system by sampling on-board sensors such as global position system (GPS) and inertial measurement

units (IMUs). Filtering and fusing noisy data from multiple sources is often accomplished through estimation techniques such as the Kalman filter.

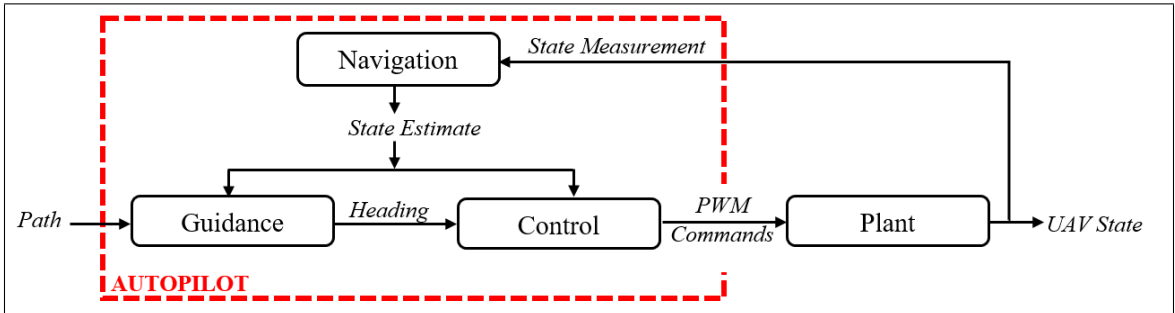


Figure 2.3: Autopilot’s Navigation, Guidance, and Control Architecture

2.3 Path Planning and Guidance

Obstacle free and flyable paths are typically pre-planned and generated off-line at a dedicated ground station using a path planner. Many methods can be used for generating paths, however the process is generally executed in two steps consisting of optimization and refinement. Optimization builds shortest path taking in constraints such as obstacles and mission objectives. The optimized path is then refined to meet a vehicle’s dynamic constraints, such as turn rate and velocity. On-board guidance systems attempt to minimize the lateral error to the path by commanding a heading pointing to the path. Guidance methods for following a pre-planned path include geometric methods such as waypoint or carrot chasing and control techniques such as proportional-integral-derivative (PID), non-linear guidance laws, and linear quadratic regulator (LQR) [20]. Due to traditional guidance method’s dependence on a path planner to construct an obstacle free and flyable path, these methods often lack a mechanism to avoid new obstacles. Re-planning and relaying a new obstacle free path may be impossible under certain conditions, such as flying beyond line-of-sight. Path planning on-board to avoid a new obstacle could be accomplished by inserting a new temporary path or by completely re-planning, however introduces several

challenges such as waypoint placement and density. It would be beneficial to include obstacle avoidance into a UAVs guidance system to remove the need to communicate with the ground station or use an on-board path planner which may be accomplished with potential field or vector field.

2.4 Potential Field

Potential field is based on the principle of artificial attractive and repulsive forces acting on a point mass that is guided to a desired goal while avoiding static and dynamic obstacles [13]. Goal states are represented as an attractive force that pulls a point mass in the direction of minimal energy while obstacles are represented as repulsive forces that act locally to push the point mass away. Potential field is also capable of acting as a path and trajectory planning algorithm [14], possibly eliminating the off-board path planner.

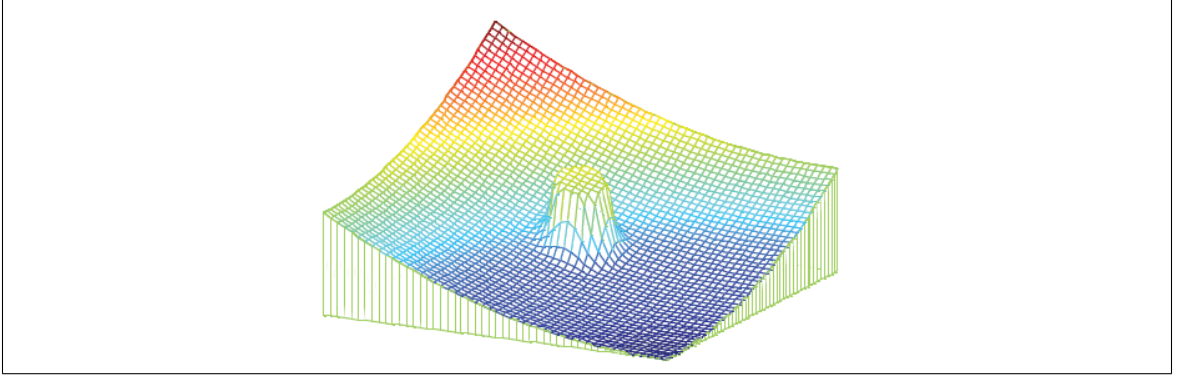


Figure 2.4: Single Obstacle Potential Field Gradient [15]

An example of potential field can be found in [16–18] which allowed for real time goal seeking with obstacle avoidance on a mobile ground robot equipped with ultrasonic sensors. The robot located at (x_0, y_0) is attracted towards a goal with constant magnitude force \vec{F}_t located at (x_t, y_t) and a distance d_t from the robot. In the immediate area of the robot, an active window exists which records integer certainty values inside discrete cells. Cells containing an obstacle provide a repulsive force $\vec{F}_{i,j}$ opposite in direction to the line-

of-sight from vehicle to cell location (x_i, y_j) , where (i, j) represents the cell index, F_{cr} is a constant repulsive force, W the vehicle's width, $C_{i,j}$ a cell's certainty, and $d_{i,j}$ the distance to the center of the cell with respect to robots center.

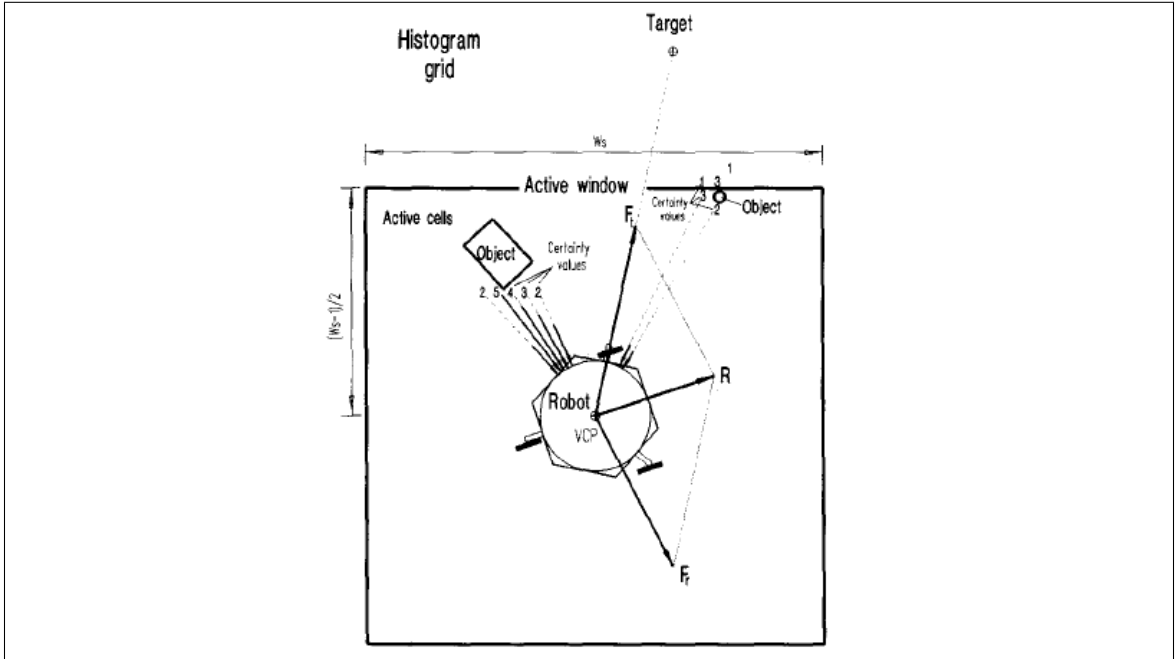


Figure 2.5: Virtual force field histogram acting on a mobile robot [17]

$$\vec{F}_{i,j} = \frac{F_{cr} W^n C_{i,j}}{d_{i,j}^n} \left(\frac{x_i - x_0}{d_{i,j}} \hat{x} + \frac{y_i - y_0}{d_{i,j}} \hat{y} \right) \quad (2.1)$$

The total repulsive force exerted on the robot is determined by summing the active cells, shown in Equation 2.2

$$\vec{F}_r = \sum_{i,j} \vec{F}_{i,j} \quad (2.2)$$

$$\vec{F}_t = F_{ct} \left(\frac{x_t - x_0}{d_t} \hat{x} + \frac{y_t - y_0}{d_t} \hat{y} \right) \quad (2.3)$$

Summing together attractive and repulsive forces produce a vector \vec{R} that can be used for heading guidance, shown in Equation 2.4.

$$\vec{R} = \vec{F}_r + \vec{F}_t \quad (2.4)$$

Major drawbacks to potential field were identified in [18] consisting of local minimum and oscillations in corridors. The local minimum problem occurs when closely spaced obstacle's potential combine to produce a well on the descent gradient where a pre-mature stable point is reached, shown in Figure 2.6. Additionally, closely spaced obstacles may also be difficult to pass between, shown in Figure 2.7a. Oscillations can also be experienced near obstacles or in narrow passages at high speeds, shown in Figure 2.7b.

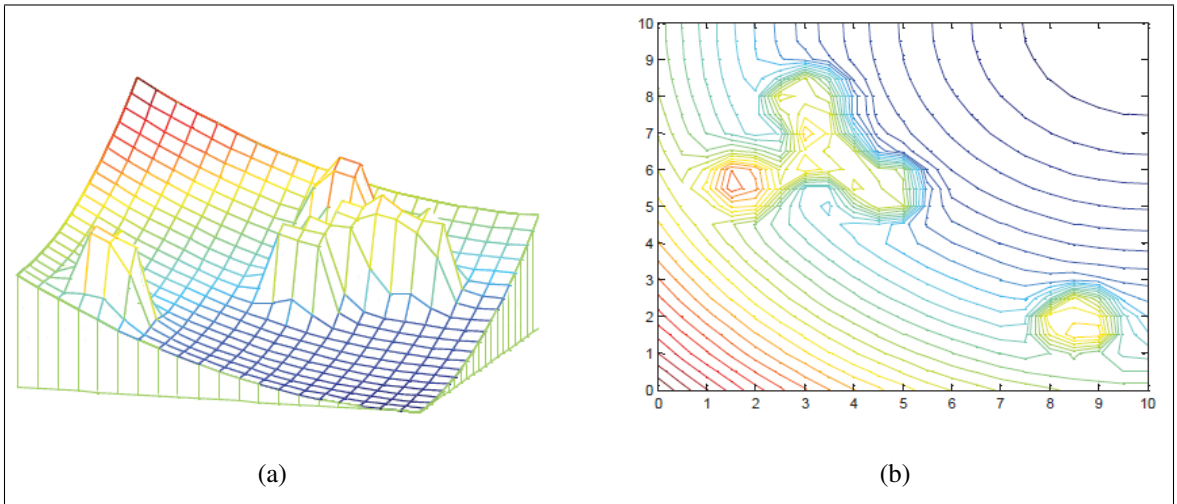


Figure 2.6: Potential Field Local Minimum [15]

Proposed solutions to local minimum include object clustering and virtual waypoint method [15], virtual escaping route [?], and use of navigation functions [19]. Oscillations in potential field were addressed in [?] and [?].

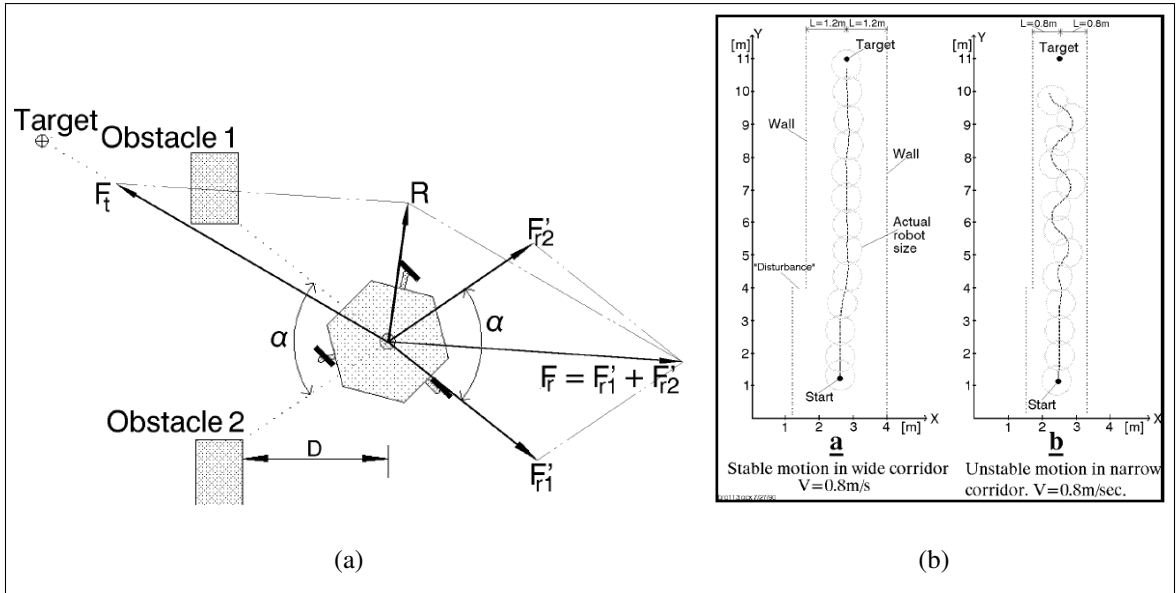


Figure 2.7: Potential Field Local Minimum [15]

Navigation functions [19] and obstacle clustering [15] have been used to prevent local minimums in potential field. Navigation functions relate kinematic constraints to the gradient potential to produce a bounded and local minimum free solution [14]. Clustering closely spaced obstacles into a single and equally repulsive obstacle prevents local minimum from forming, shown in Figure 2.8.

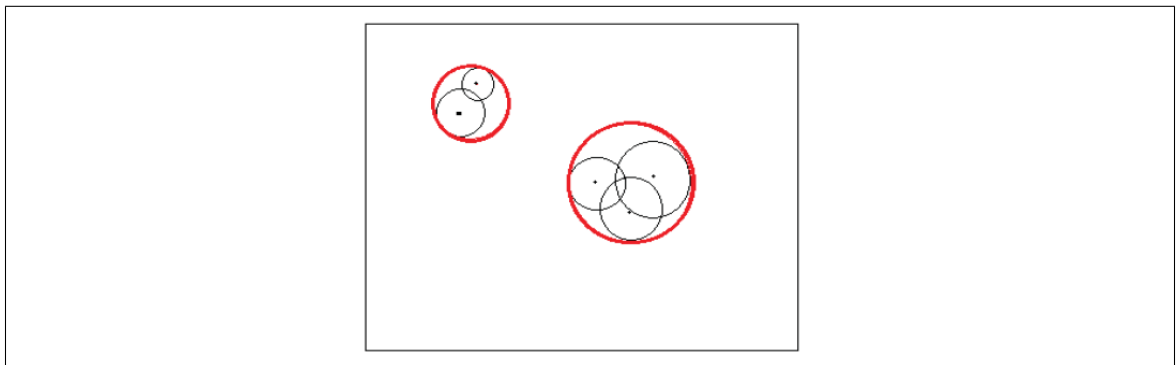


Figure 2.8: Obstacle Clustering [15]

Potential Field's ability to avoid obstacles and combine path planning, trajectory planning, and control into a single computationally inexpensive system makes it an attractive motion control system for robots seeking a singular point, even with the limitations discussed in [18].

In addition to local minimum and oscillations, potential field may not be ideal for providing guidance to return to a sensor path after avoiding an obstacle. Unlike the mobile ground robots in [16], fixed wing UAVs must maintain a minimum forward velocity, have limited turning radius, and cannot converge to a single point. Vehicles with velocity and turn rate constraints may not return to a pre-planned path once the obstacle has been avoided. Vector fields that direct a UAV to paths connecting waypoints have been developed using Lyapunov and gradient vector field techniques.

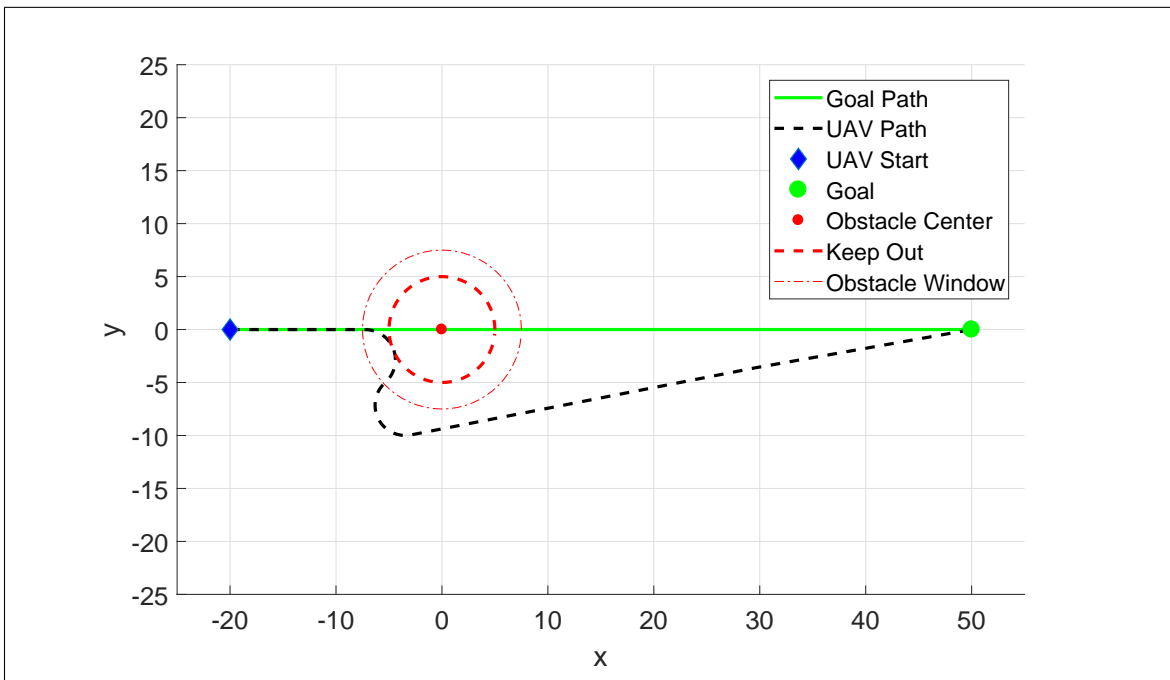


Figure 2.9: UAV avoiding obstacle with VFF Guidance

2.4.1 Path Following Vector Field Guidance

Path following can be accomplished with vector fields which produce a heading guidance that asymptotically converges and circulates a path. A comparison between vector field and waypoint guidance techniques was presented in [20] where each method was evaluated based on its complexity, robustness, and accuracy. Vector field produced guidance that was both robust to external wind disturbances while maintaining a low cross track error.

The UAV guidance system is responsible for taking high level pre-planned paths from the ground station and providing a reference heading command to the control system. Several methods for path following guidance were investigated in [20] consisting of carrot chasing [21], non-linear guidance law, pure line-of-sight [22], linear quadratic regulator [23], and vector field method [24]. A Monte Carlo simulation with wind disturbances was conducted for the guidance methods above in [20] to determine each method's performance based on accuracy, robustness, and control effort. The vector field method followed the path with the least tracking error and control effort which is the primary goal of path following.

2.5 Vector Field Guidance

2.5.1 Introduction to Vector Field Guidance

Vector Field is a guidance and control approach that can be used to transition a robotic system from an initial state to a final state. Final states, or goals, act as artificial attractive forces that pull on the robotic system while obstacles act as artificial repulsive forces that push the robotic system away. Classes of vector fields can be categorized as point seeking or path following algorithms. Potential Field and Virtual Force Field (VFF) methods converge to a single point and avoid obstacles by applying artificial attractive and repulsive forces. Lyapunov and Gradient Vector Fields provide guidance that asymptotically converges and follows a path. Obstacle avoidance has been achieved

with Gradient Vector Fields by assigning repulsive weights to a convergence term. Weights currently act as a high level specification of the desired guidance behavior and may be further optimized.

2.5.2 Lyapunov Vector Fields

Lyapunov vector fields for converging and following straight and circular paths were described in [24]. For converging and following a straight path, a guidance vector χ^d is determined in Equation 2.5, where χ^∞ is the course approach angle, y is the lateral distance to the path, and k is a positive constant that determines the rate of transition between convergence and following. An example of a Lyapunov vector field converging and following a straight line is shown in Figure ??a.

$$\chi^d(y) = -\chi^\infty \frac{2}{\pi} \tan^{-1}(ky) \quad (2.5)$$

For converging and following a circular path, a guidance vector χ^d is determined in Equation 2.6, where γ is the UAVs angular position with respect to the circle, r is the paths radius, d is the distance from the circles center, and k is a positive constant that determines the transition behavior. An example of a Lyapunov vector field for converging and following a circular path is shown in Figure ??b.

$$\chi^d(d) = \gamma - \frac{\pi}{2} - \tan^{-1}\left(k \frac{d-r}{r}\right) \quad (2.6)$$

Straight and circular path vector fields can be selectively activated throughout flight to form more complex paths, shown in [24–27]. Lyapunov vector field for curved path following was presented in [28] which may allow for more complex paths and eliminates the need to switch between vector fields.

Straight and circular path vector fields can be selectively activated throughout flight to form more complex paths, shown in [24–27] and Figure 2.11.

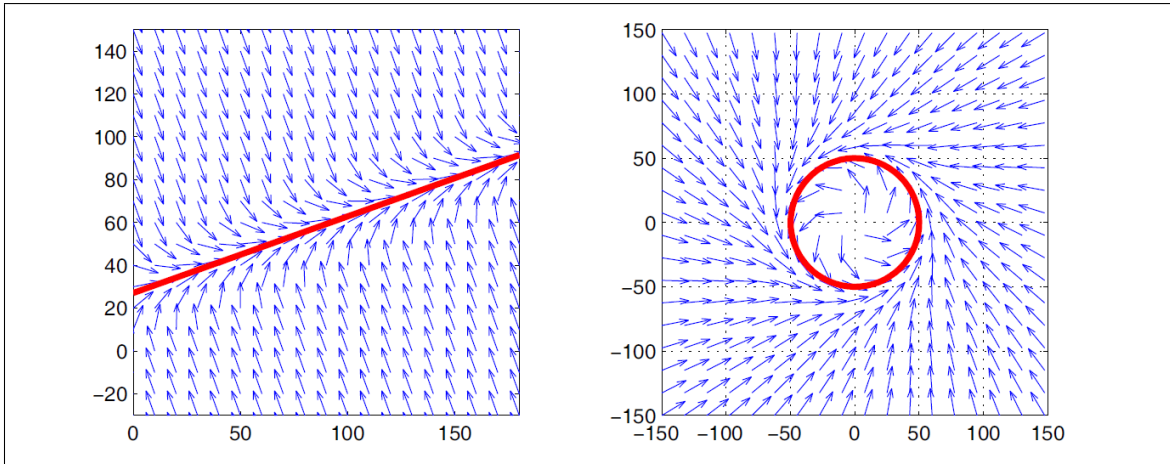


Figure 2.10: Lyapunov vector field for straight line and circular primitives [24]

Each path primitive has a vector field associated with it and determining which field to use can be approached in two different ways.

Fields from all of the primitives can be summed together similar to the attractive and repulsive forces in potential field.

Second, fields can be selectively activated and deactivated based on the position of the UAV.

Summing together vector fields, as pointed out in [24], can result in several problems including dead zones, sinks, and singularities.

Selectively activating each vector field as a UAV nears waypoints was used in [24–27].

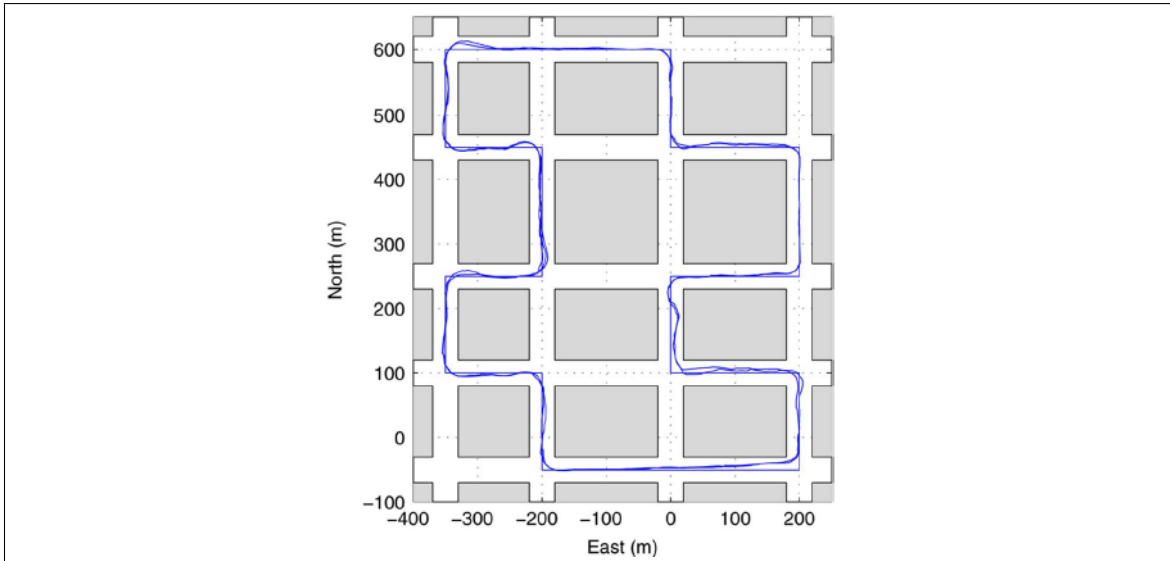


Figure 2.11: Straight path following in urban environment [24] using Lyapunov Vector Field

Lyapunov Vector field construction for curved paths was presented in [28] and is shown in Figure 2.12. Constructing a Vector Field for an arbitrary curve may allow for more complex paths and could eliminate the need for switching between primitives.

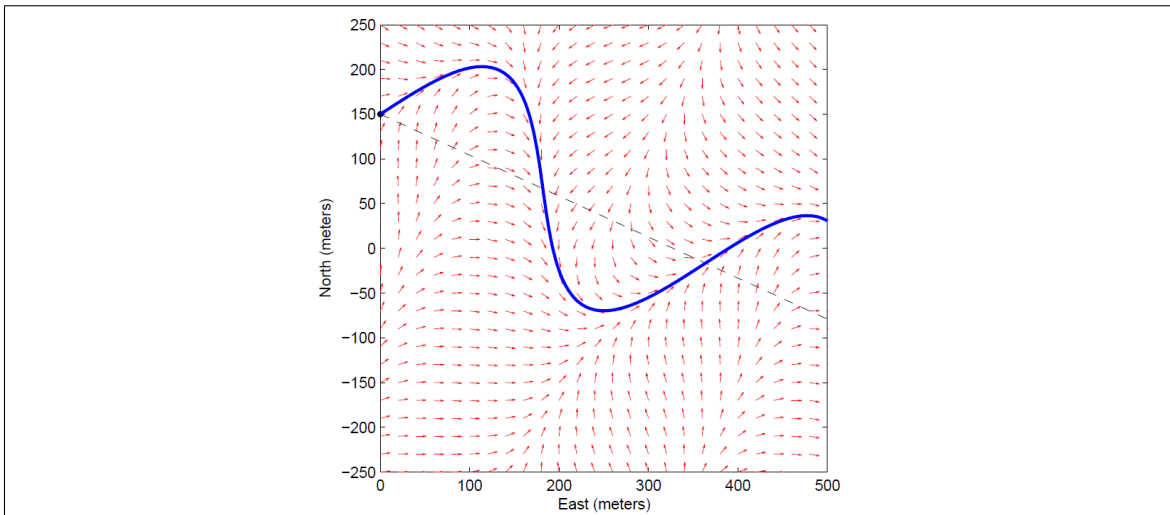


Figure 2.12: Lyapunov vector field approach curved path asymptotically [28]

Primitive circular vector fields were modified in [29, 30] via non-linear coordinate transformations to produce elliptical 2.13a, or racetrack 2.13b, fields. Transforming the circular field as a function of a Kalman filter's covariance matrix when sensing an unknown target was investigated in [30].

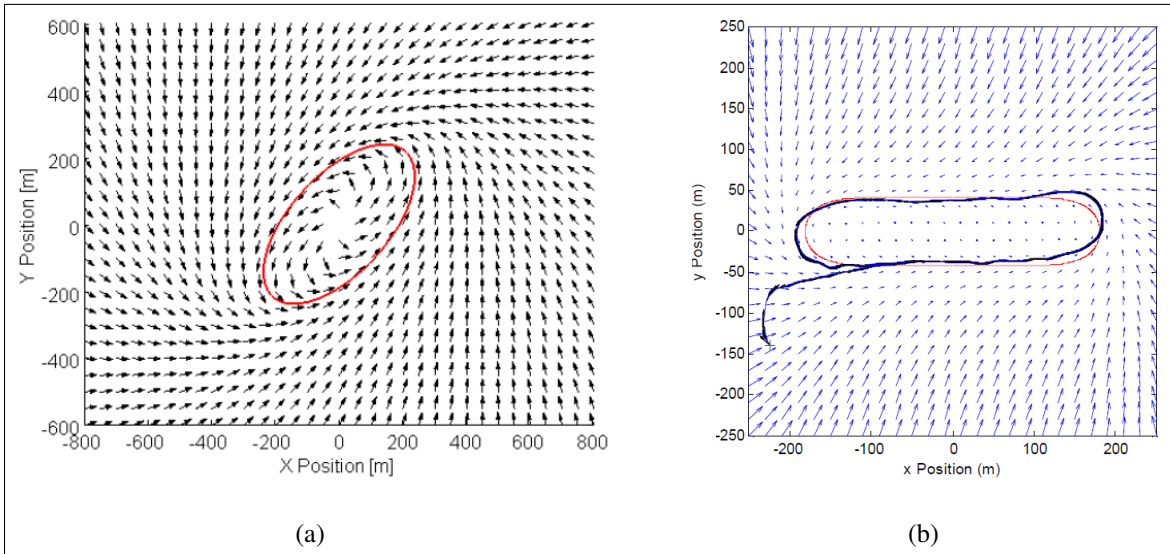


Figure 2.13: Elliptical VF produced by non-linear coordinate transformations a) [30] and b) [29]

Target tracking Tangent Plus Lyapunov Vector Field (TPLVF) was introduced in [31] that produced shorter paths compared to Lyapunov alone. Outside of the standoff circle, tangent vectors provided the shortest distance to a standoff circle. Inside the standoff circle, no tangent lines exist and Lyapunov was used in its place. Figure 2.14 shows the difference in paths taken for Lyapunov and tangent vector fields outside the standoff circle. The TPLVF was later used for path planning to avoid obstacles in [32] while [33] constructed a tangent vector field for curved paths.

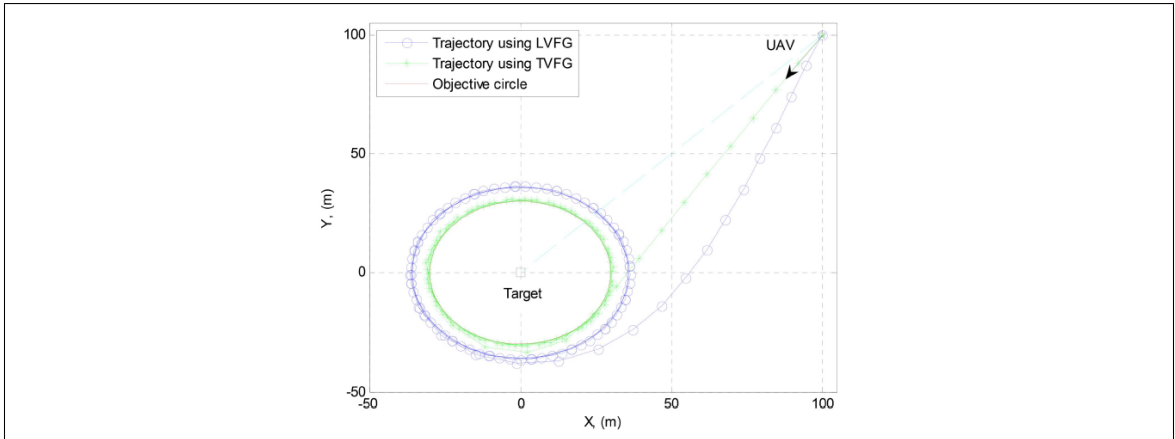


Figure 2.14: Tangent plus lyapunov vector fields for shortest path target tracking [32]

2.5.3 Path Planning Vector Fields

All methods that consider obstacles thus far built a vector field that guides the UAV to an obstacle free path. Another approach is to use vector fields as a high level specification for heuristic path planning algorithms [34]. An optimal Rapid Random Trees (RRT*) algorithm used a vector field as a guide to explore the configuration space of the UAV for an obstacle free path. Branches extend from the root, or initial location of the UAV, randomly throughout the map with a finite deviation from the initial vector field. When a branch encounters an obstacle it is trimmed and no longer explored. The path of minimum cost, or least distance, is selected for the UAV to use as a reference path. An example of the algorithm is shown in Figure 2.15.

A Vector Field was constructed inside a configuration space with edges defined by Delaunay triangulation (DT) in [35]. A simulation of a robot traversing a vector field inside a set of DTs can be seen in Figure 2.16. Vector fields designed to stay inside a region of DTs may be used with optimal path planning algorithms for navigating urban environments [36].

So far all of the vector field methods discussed have avoided obstacles by planning paths around them. Paths are typically calculated at the ground station and if

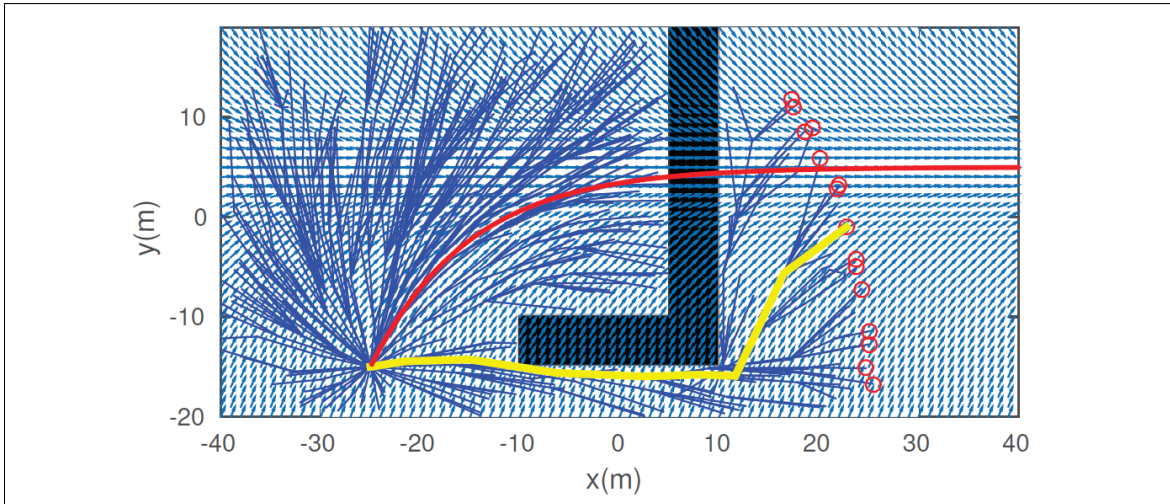


Figure 2.15: RRT* path planner with a VF used as a task specification [34]

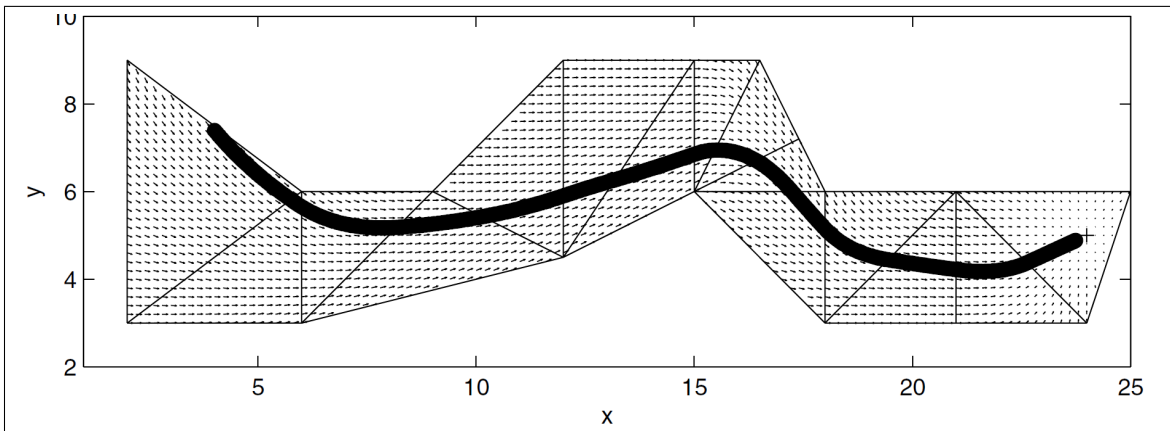


Figure 2.16: Vector field within a set of delaunay triangles [35]

communication is lost a new path may not be relayed to a UAV encountering a new obstacle. A possible solution is using vector fields to provide a repulsive force such as that seen in [2, 3, 37].

2.5.4 Gradient Vector Field

The Gradient Vector Field (GVF) method produces a similar field to LVF, however has several advantages over LVFs. GVF produces an n -dimensional vector field that

converges and circulates to both static and time varying paths [38]. Additionally, convergence, circulation, and time-varying terms that make up the GVF are decoupled from each other allowing for easy weighting of the total field [39]. GVFs converge and circulate at the intersection, or level set, of $n - 1$ dimensional implicit surfaces ($\alpha_i : \mathbb{R}^n \rightarrow \mathbb{R} | i = 1, \dots, n - 1$). The integral lines of the field are guaranteed to converge and circulate the level set when two conditions are met: 1) the implicit surface functions are positive definite and 2) have bounded derivatives. Consider the space with dimensions in set \mathbf{q} :

$$\mathbf{q} = \begin{bmatrix} x_1, x_2, \dots, x_n \end{bmatrix} \quad (2.7)$$

The total vector field \vec{V} is calculated by:

$$\vec{V} = G\nabla V + H \wedge_{i=1}^{n-1} \nabla_q \alpha_i - LM(\alpha)^{-1}a(\alpha) \quad (2.8)$$

or in component form:

$$\vec{V} = \vec{V}_{conv} + \vec{V}_{circ} + \vec{V}_{tv} \quad (2.9)$$

where \vec{V}_{conv} produces vectors perpendicular to the path, \vec{V}_{circ} produces vectors parallel to the path, and \vec{V}_{tv} is a feed-forward term that produces vectors accounting for a time varying path. The scalars G, H , and L weight convergence, circulation, and time varying components respectively.

Convergence is calculated by:

$$\vec{V}_{conv} = G\nabla V \quad (2.10)$$

where scalar G is multiplied by the gradient of the definite potential function V :

$$V = -\sqrt{\alpha_1^2 + \alpha_2^2} \quad (2.11)$$

Circulation is calculated by taking the wedge product of the gradient:

$$\vec{V}_{circ} = \wedge_{i=1}^{n-1} \nabla_q \alpha_i \quad (2.12)$$

In the case of ($n = 3$) the wedge product simplifies as the cross product:

$$\vec{V}_{circ} = \nabla_q \alpha_1 \times \nabla_q \alpha_2 \quad (2.13)$$

The feed-forward time-varying component is calculated by:

$$\vec{V}_{tv} = M^{-1} a \quad (2.14)$$

where,

$$M = \begin{bmatrix} \nabla \alpha_1^T \\ \nabla \alpha_2^T \\ (\nabla \alpha_1 \times \nabla \alpha_2)^T \end{bmatrix} \quad (2.15)$$

$$a = \begin{bmatrix} \frac{\partial \alpha_1}{\partial t} & \frac{\partial \alpha_2}{\partial t} & 0 \end{bmatrix}^T \quad (2.16)$$

In [38–40] holonomic robots were modeled as a single integrator $\dot{q} = h$, where h acted as an input calculated from a GVF. Constant speed u was controlled by calculating weighting scalars that maintained the condition $\|\dot{q}\| = u$. Other studies normalized the vector \vec{V} and used it as a heading guidance while assuming velocity is held constant by the autopilot [2, 41]. Assuming velocity is controlled by a separate system frees up the vector field scalars to modify field behavior for other applications, such as obstacle avoidance.

The standoff tracking and avoidance scenario presented in [2] used GVF as a heading guidance and static GVF weights to specify high level guidance behavior. A fixed UAV was tasked with loitering around a slow moving ground target while avoiding obstacles. A circular attractive vector field was attached to a moving ground target and

summed with repulsive vector fields centered at the obstacles. The strength of repulsive obstacle fields were weighted by the hyperbolic tangent decay function in Equation 2.17, where d is the range to the obstacle and R is the radius of the decay.

$$P = R \frac{\tanh(2\pi d - \pi) + 1}{2} \quad (2.17)$$

The performance of Lyapunov [21] and gradient vector field [38–40] were compared for their cross track error with respect to the loiter circle. Gradient vector field had favorable performance due to compensation for a time-varying vector field. The path of the fixed wing UAV tracking a slow moving ground target while avoiding static obstacles is shown in Figure 2.17

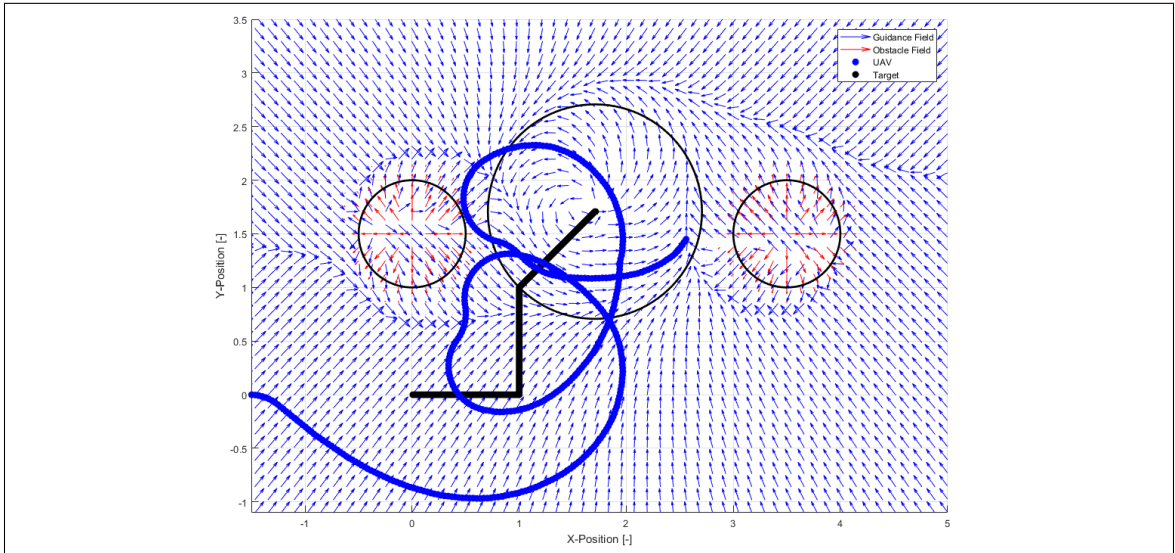


Figure 2.17: Place holder image of UAV following ground target [2]

Summing attractive and repulsive vector fields may result in null guidance where the fields cancel, providing no guidance. The presence of singularities were not addressed in [2], mentioned briefly in [24] and observed in [3]. For fixed wing UAVs the lack of guidance may prevent the UAV from avoiding an obstacle, while multi-rotor UAVs may end up in a trap situation. Singularities may be present at any location where a goal field

and obstacle field are of equal strength. Detecting singularities and modifying the GVF for an improved obstacle avoidance is the contribution of this research.

2.6 Dubins Vehicle

The dynamics of UAVs are often simplified when simulating guidance systems by modeling the UAV as a Dubin's vehicle [24–26, 28, 30]. It is assumed that the autopilots control system is capable of maintaining stability, speed u , and can turn the vehicle at a fixed turn rate $\dot{\theta}$. The position of the UAV \vec{X} at time t is calculated from the integral of the velocity vector \vec{U} , Equation 2.19. Heading is an input from a guidance system, such as waypoint, potential field, or vector field.

$$\vec{U}(t) = u \begin{bmatrix} \cos(\theta(t)) \\ \sin(\theta(t)) \end{bmatrix} \quad (2.18)$$

$$\vec{X}(t) = \vec{U}dt + \vec{X}(t - 1) \quad (2.19)$$

$$\dot{\theta} \leq 20deg/s \quad (2.20)$$

2.7 Unmanned Aerial Vehicle Simulation

Testing new guidance, navigation, and control algorithms on flight hardware can be costly, require significant time, and requires an adequately large airspace. Before spending the time to reserve airspace and allocate man hours for flight tests it is important to test algorithms in a controlled environment. One way to accomplish testing without actual flight is through validation through mobile robots simulating fixed wing constraints [42], [43], [44]. Vector fields have been used in robot platforms other than UAVs, including ground [45] and marine [46].

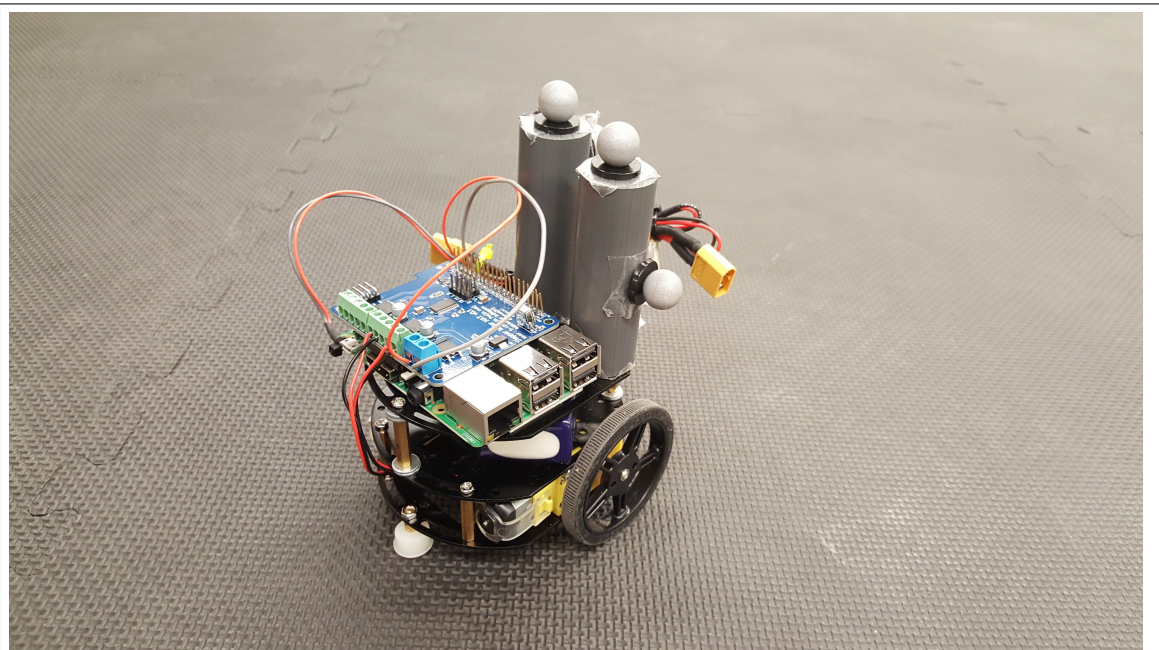


Figure 2.18: Differential drive mobile robot simulating fixed wing UAV Dubins constraints

2.8 Literature Review Summary

Vector fields can provide guidance and control for robots through the use of artificial attractive and repulsive forces. Converging to a singular point while avoiding obstacles can be achieved with Potential Field or Virtual Force Field methods. Fixed wing UAVs

cannot converge to a singular point therefore vector fields that asymptotically converge and follow a path is beneficial. Lyapunov and Gradient Vector Fields have been used for path following, standoff tracking, and obstacle avoidance. Gradient Vector Field provides convenient and decoupled access to scalar multiplicative weights for the convergence, circulation, and time-varying terms. Negative weights can be used for obstacle avoidance, however have so far been used only as high level specification of guidance behavior. Specifying vector field weights as functions of a UAV's state may enable an optimal guidance for obstacle avoidance. Validation of a modified GVF guidance can be performed on mobile ground robots simulating UAV dynamics.

3 METHODOLOGY

3.1 Introduction to Methodology

3.2 Phase I

Phase I. Demonstration of vector field trap situations and vector field singularities

Consists of path following vector field guidance summed with obstacle field

Intersecting two flat planes ($\alpha_1 = z, \alpha_2 = x$), shown in Figure 3.1 produces a GVF that converges and circulates a straight path.

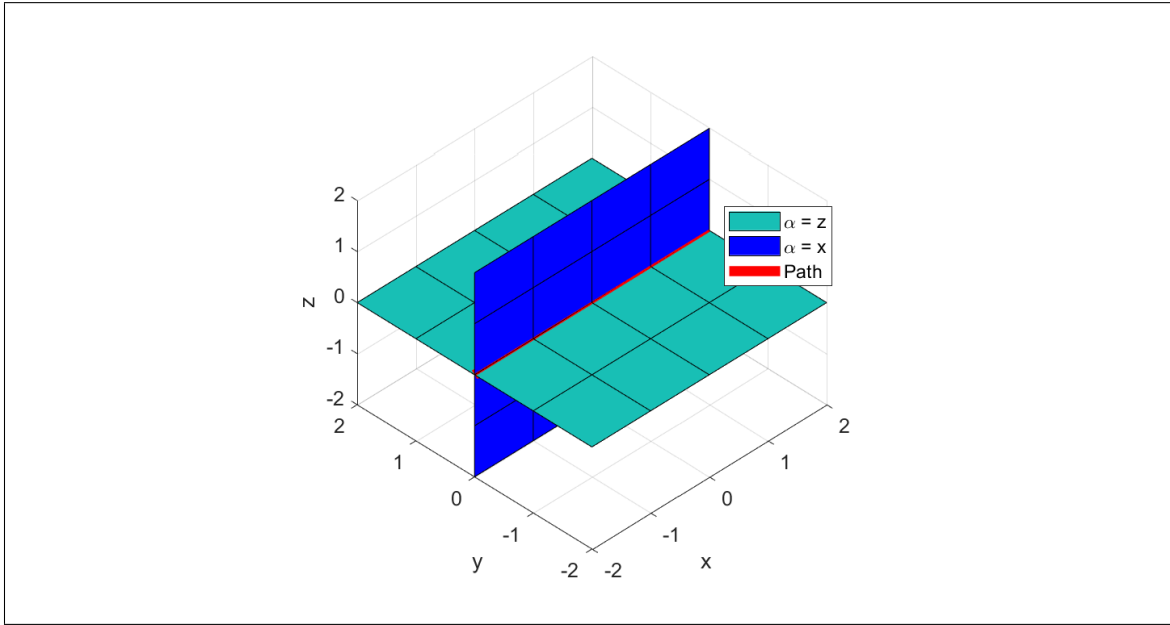


Figure 3.1: Place Intersection

How quickly the path following field transitions from convergence to circulation depends on the field weights. Equal parts convergence and circulation are shown in Figure 3.2a ($G = H = 1$) and a larger circulation value in Figure 3.2b ($G = 1, H = 5$).

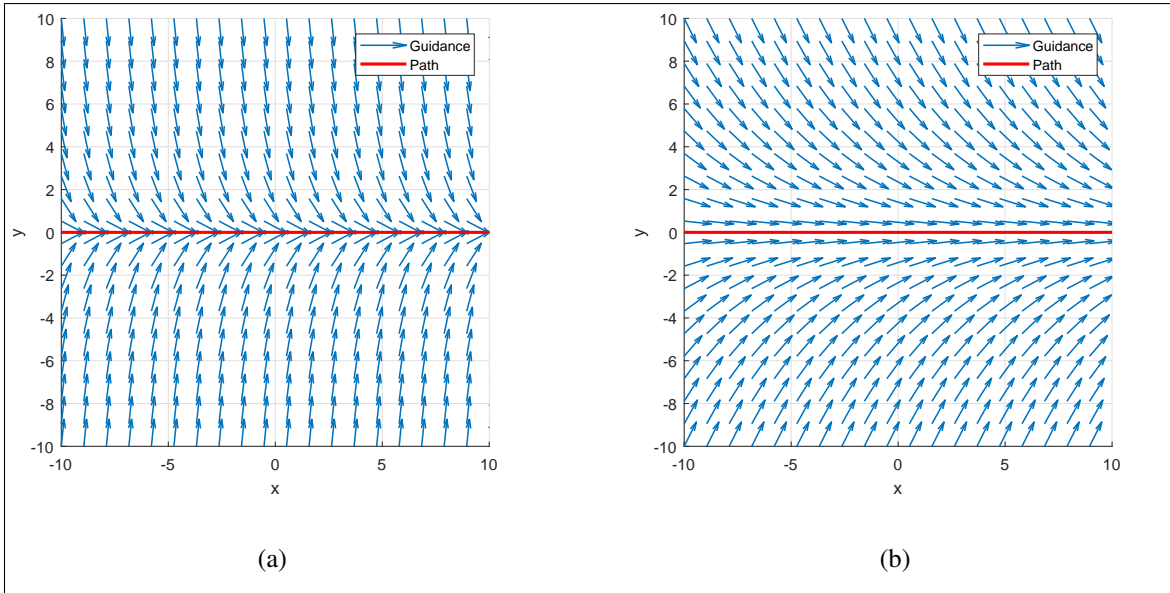


Figure 3.2: GVF converging and a) small circulation b) large circulation

A GVF for converging and following a circular path can be produced by intersecting a plane and a cylinder ($\alpha_1 = z$, $\alpha_2 = x^2 + y^2 - r^2$), shown in Figure 3.3.

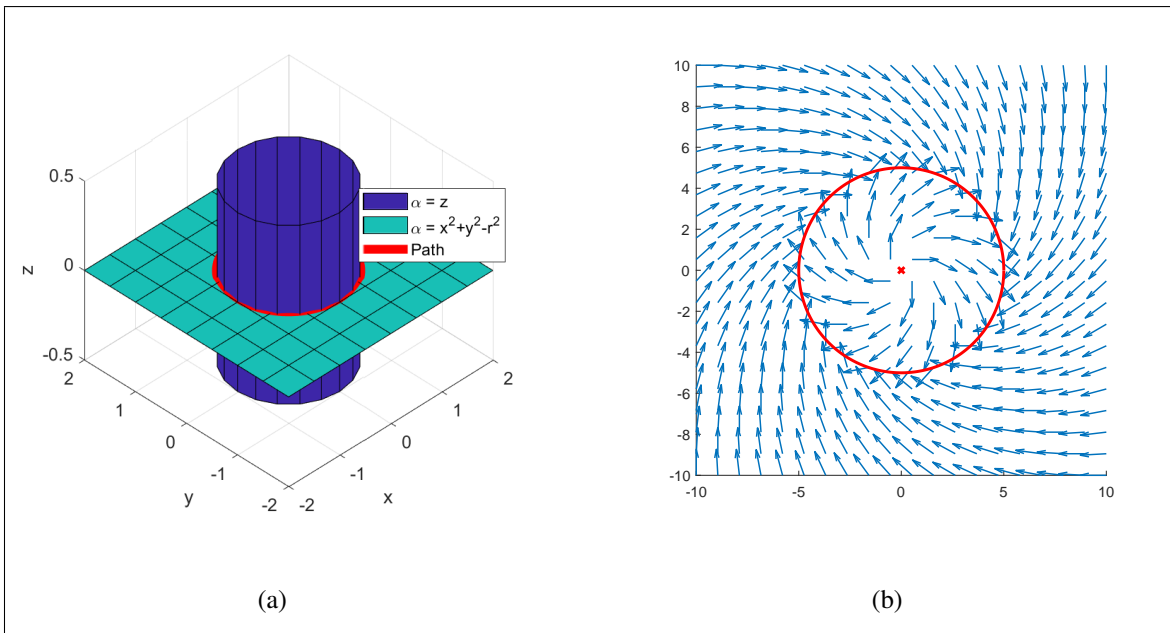


Figure 3.3: GVF converging and circulating circular path

Static paths do not require the time-varying term of the vector field calculation and can be considered zero in such cases.

Evaluating equation 2.10 for a cylinder intersecting a plane results in a vector field that converges to a circular path shown in Figure 3.4a. Note that the vectors are not of equal length for the entire configuration space, decaying in strength when approaching the curve. Normalizing the field was done in [2, 39, 40] to allow for convenient weighting of each term at a later process. The normalized convergence field for a circular path is shown in Figure 3.4b.

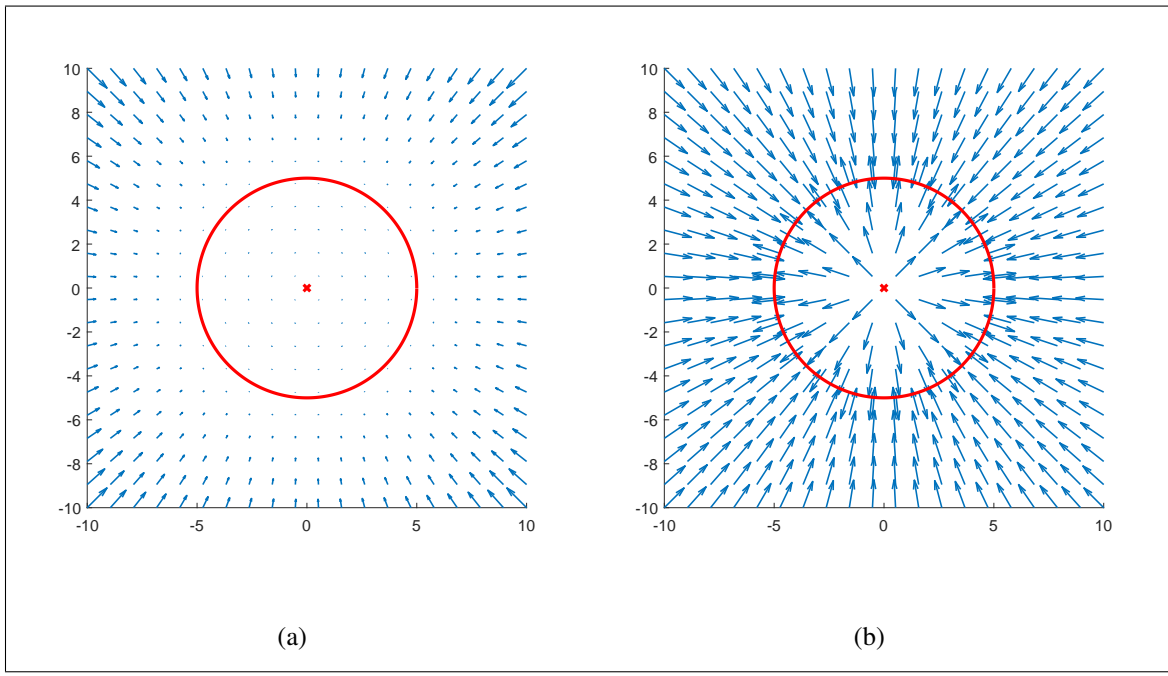


Figure 3.4: GVF circular attractive field without normalization (a) and with normalization (b)

The circulation term is calculated by taking the wedge product of each surface's gradient, shown in Equation 3.1. For surfaces in \mathbb{R}^3 , the wedge product can be simplified to the cross product shown in Equation 3.2.

$$\vec{v}_{circ} = \wedge_{i=1}^{n-1} \nabla_q \alpha_i \quad (3.1)$$

$$\vec{v}_{circ} = \nabla_q \alpha_1 \times \nabla_q \alpha_2 \quad (3.2)$$

Evaluating the circulation term results in a vector field that is parallel to a circular path, shown in Figure 3.5a. The field is normalized to produce a field with equal length vectors for the configuration space which is shown in Figure 3.5b.

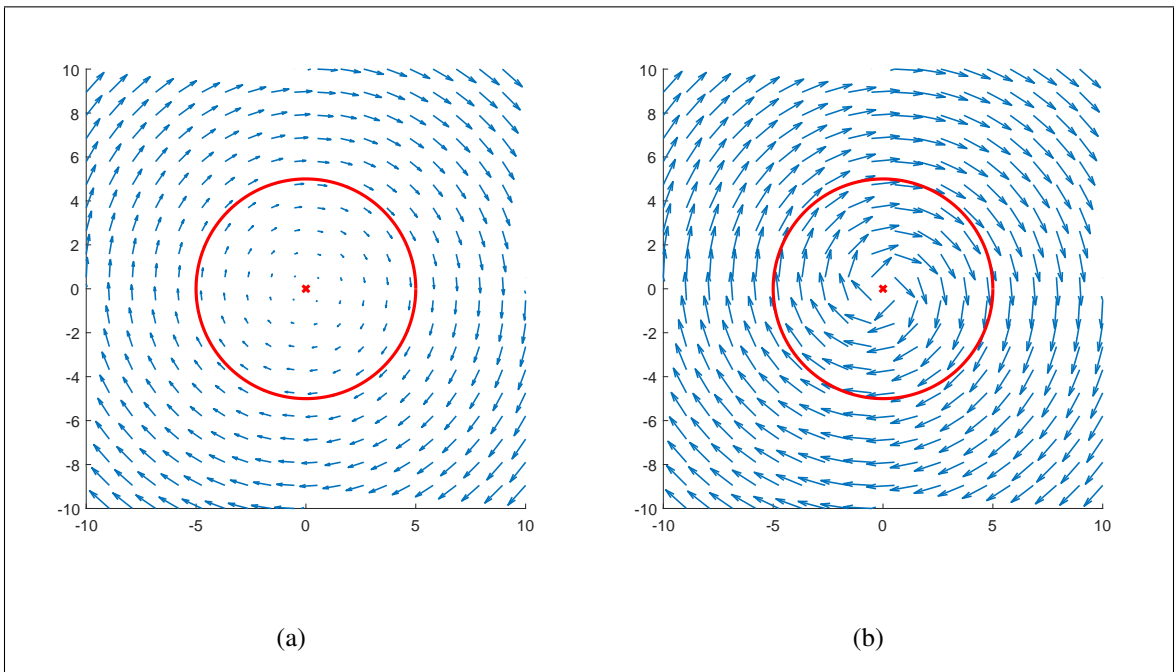


Figure 3.5: Circular GVF without normalization (a) and with normalization (b)

For dynamic paths that vary in time t , feedforward compensation is accomplished by calculating the time-varying term. The time-varying field \vec{v}_t is calculated by multiplying the inverse of a gradient matrix M with the column vector a shown in Equations 3.4 and 3.5 respectively. The resulting vector field for a circular path moving in the positive x direction can be shown in Figure 3.6a and the normalized version in Figure 3.6b.

$$\vec{v}_{tv} = M^{-1}a \quad (3.3)$$

$$M = \begin{bmatrix} \nabla \alpha_1^T \\ \nabla \alpha_2^T \\ (\nabla \alpha_1 \times \nabla \alpha_2)^T \end{bmatrix} \quad (3.4)$$

$$a = \begin{bmatrix} \frac{\partial \alpha_1}{\partial t} & \frac{\partial \alpha_2}{\partial t} & 0 \end{bmatrix}^T \quad (3.5)$$

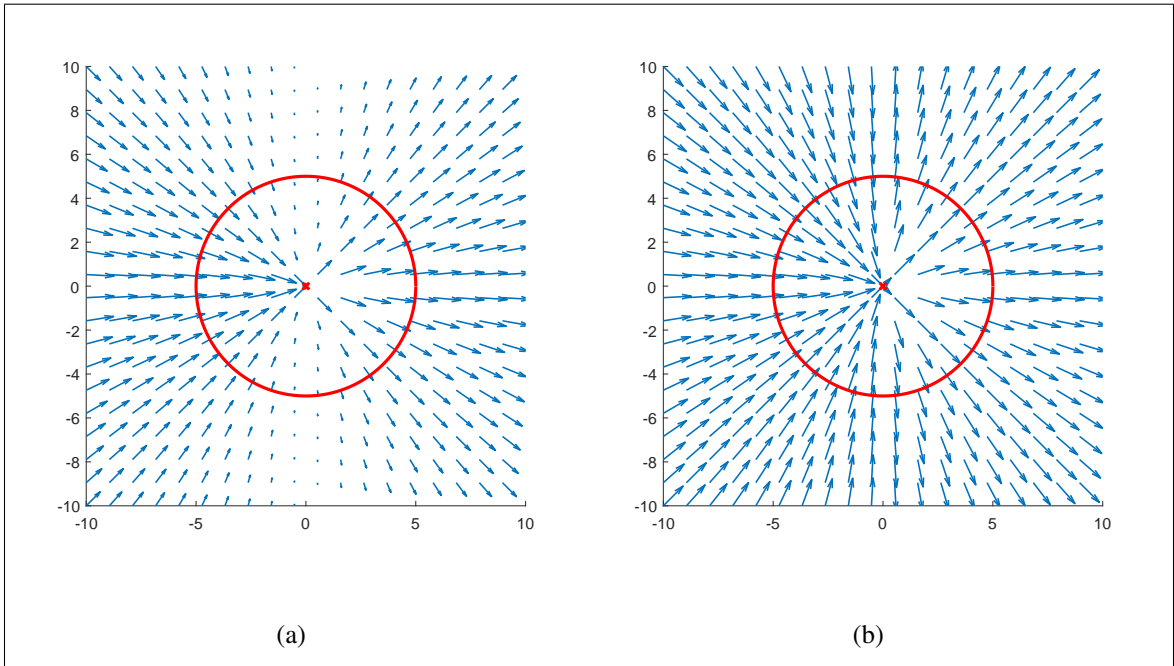


Figure 3.6: Circular time-varying GVF without normalization (a) and with normalization

(b)

Summing together the normalized convergence, circulation, and time-varying terms results in the total normalized and weighted field field \vec{V} shown defined in Equation 3.6. Scalar weights, (G, H, L) , are added after normalization to increase or decrease the contribution of convergence, circulation, and time-varying respectively.

$$\vec{V} = \mathbf{G}\|\vec{v}_{conv}\| + \mathbf{H}\|\vec{v}_{circ}\| + \mathbf{L}\|\vec{v}_{tv}\| \quad (3.6)$$

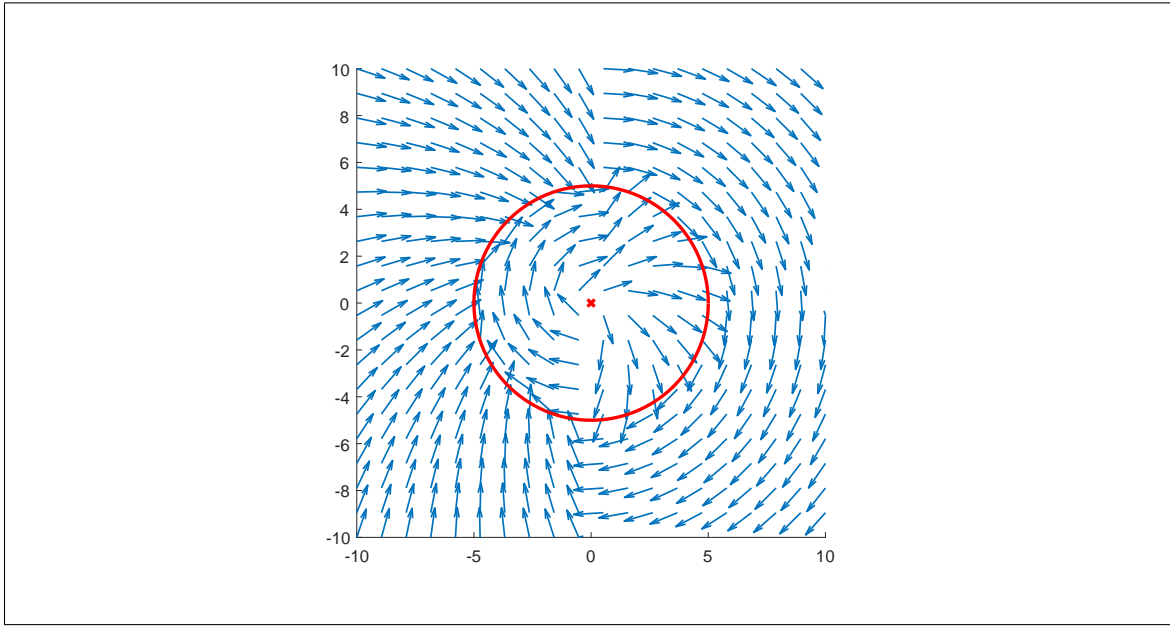


Figure 3.7: GVF with unity ($\mathbf{G}=\mathbf{H}=\mathbf{L}=\mathbf{I}$) weights for a moving circular path

- Field Construction
- Straight Path
- Circular path
- obstacle definition
- Obstacle Field
- Field decay radius definition
- tanh function
- repulsive and repulsive+circulation side-by-side

3.3 Phase II

3.4 Phase III

4 RESULTS

4.1 Introduction to Results

4.2 Phase I

4.3 Phase II

4.4 Phase III

5 CONCLUSIONS

6 FUTURE WORK

REFERENCES

- [1] Bone, E., “UAVs backbound and issues for congress.pdf,” 2003.
- [2] Wilhelm, J. P., Wambold, G., and Clem, G., “Vector field avoidance,” *ICUAS*, 2018.
- [3] Panagou, D., “Motion planning and collision avoidance using navigation vector fields,” *Robotics and Automation (ICRA), 2014 IEEE International Conference on*, IEEE, 2014, pp. 2513–2518.
- [4] Ariyur, K. B. and Fregene, K. O., “Autonomous tracking of a ground vehicle by a UAV,” *American Control Conference*, 2008, IEEE, 2008, pp. 669–671.
- [5] Teuliere, C., Eck, L., and Marchand, E., “Chasing a moving target from a flying UAV,” *Intelligent Robots and Systems (IROS), 2011 IEEE/RSJ International Conference on*, IEEE, 2011, pp. 4929–4934.
- [6] Oh, H., Kim, S., Shin, H.-S., Tsourdos, A., and White, B., “Coordinated standoff tracking of groups of moving targets using multiple UAVs,” *Control & Automation (MED), 2013 21st Mediterranean Conference on*, IEEE, 2013, pp. 969–977.
- [7] Hyondong Oh, Seungkeun Kim, Hyo-sang Shin, and Tsourdos, A., “Coordinated standoff tracking of moving target groups using multiple UAVs,” *IEEE Transactions on Aerospace and Electronic Systems*, Vol. 51, No. 2, April 2015, pp. 1501–1514.
- [8] Ulun, S. and Unel, M., “Coordinated motion of UGVs and a UAV,” *Industrial Electronics Society, IECON 2013-39th Annual Conference of the IEEE*, IEEE, 2013, pp. 4079–4084.
- [9] Beard, R. W. and McLain, T. W., *Small unmanned aircraft: theory and practice*, Princeton University Press, Princeton, N.J, 2012, OCLC: ocn724663112.
- [10] Choi, H., Geeves, M., Alsalam, B., and Gonzalez, F., “Open source computer-vision based guidance system for UAVs on-board decision making,” *Aerospace Conference, 2016 IEEE*, IEEE, 2016, pp. 1–5.
- [11] Martnez, C., Mondragn, I. F., Olivares-Mndez, M. A., and Campoy, P., “On-board and Ground Visual Pose Estimation Techniques for UAV Control,” *Journal of Intelligent & Robotic Systems*, Vol. 61, No. 1-4, Jan. 2011, pp. 301–320.
- [12] Yamasaki, T., Balakrishnan, S. N., and Takano, H., “Integrated guidance and autopilot for a path-following UAV via high-order sliding modes,” *American Control Conference (ACC), 2012*, IEEE, 2012, pp. 143–148.
- [13] Khatib, O., “Real-time obstacle avoidance for manipulators and mobile robots,” *The international journal of robotics research*, Vol. 5, No. 1, 1986, pp. 90–98.

- [14] Rimon, E., “Exact Robot Navigation Using Artificial Potential Functions.pdf,” 1992.
- [15] Liu, Y. and Zhao, Y., “A virtual-waypoint based artificial potential field method for UAV path planning,” *Guidance, Navigation and Control Conference (CGNCC), 2016 IEEE Chinese*, IEEE, 2016, pp. 949–953.
- [16] Borenstein, J. and Koren, Y., “Real-time obstacle avoidance for fast mobile robots in cluttered environments,” *Robotics and Automation, 1990. Proceedings., 1990 IEEE International Conference on*, IEEE, 1990, pp. 572–577.
- [17] Borenstein, J. and Koren, Y., “The vector field histogram-fast obstacle avoidance for mobile robots,” *IEEE transactions on robotics and automation*, Vol. 7, No. 3, 1991, pp. 278–288.
- [18] Koren, Y. and Borenstein, J., “Potential Field Methods and their inherent limitations for mobile robot navigation.pdf,” 1991.
- [19] Goerzen, C., Kong, Z., and Mettler, B., “A Survey of Motion Planning Algorithms from the Perspective of Autonomous UAV Guidance,” *Journal of Intelligent and Robotic Systems*, Vol. 57, No. 1-4, Jan. 2010, pp. 65–100.
- [20] Sujit, P., Saripalli, S., and Sousa, J. B., “Unmanned Aerial Vehicle Path Following: A Survey and Analysis of Algorithms for Fixed-Wing Unmanned Aerial Vehicles,” *IEEE Control Systems*, Vol. 34, No. 1, Feb. 2014, pp. 42–59.
- [21] Manjunath, A., Mehrok, P., Sharma, R., and Ratnoo, A., “Application of virtual target based guidance laws to path following of a quadrotor UAV,” IEEE, June 2016, pp. 252–260.
- [22] Fortuna, J. and Fossen, T. I., “Cascaded line-of-sight path-following and sliding mode controllers for fixed-wing UAVs,” *Control Applications (CCA), 2015 IEEE Conference on*, IEEE, 2015, pp. 798–803.
- [23] Capello, E. and Tempo, R., “A simulation-based approach for control design of uncertain UAVs,” *Decision and Control (CDC), 2012 IEEE 51st Annual Conference on*, IEEE, 2012, pp. 3086–3091.
- [24] Nelson, D. R., “Cooperative control of miniature air vehicles,” 2005.
- [25] Nelson, D. R., Barber, D. B., McLain, T. W., and Beard, R. W., “Vector field path following for small unmanned air vehicles,” *American Control Conference, 2006*, IEEE, 2006, pp. 7–pp.
- [26] Nelson, D., Barber, D., McLain, T., and Beard, R., “Vector Field Path Following for Miniature Air Vehicles,” *IEEE Transactions on Robotics*, Vol. 23, No. 3, June 2007, pp. 519–529.

- [27] Jung, W., Lim, S., Lee, D., and Bang, H., “Unmanned Aircraft Vector Field Path Following with Arrival Angle Control,” *Journal of Intelligent & Robotic Systems*, Vol. 84, No. 1-4, Dec. 2016, pp. 311–325.
- [28] Griffiths, S., “Vector Field Approach for Curved Path Following for Miniature Aerial Vehicles,” American Institute of Aeronautics and Astronautics, Aug. 2006.
- [29] Frew, E., “Lyapunov Guidance Vector Fields for Unmanned Aircraft Applications.pdf,” .
- [30] Frew, E. W., “Cooperative standoff tracking of uncertain moving targets using active robot networks,” *Robotics and Automation, 2007 IEEE International Conference on*, IEEE, 2007, pp. 3277–3282.
- [31] Chen, H., Chang, K., and Agate, C. S., “Tracking with UAV using tangent-plus-Lyapunov vector field guidance,” *Information Fusion, 2009. FUSION'09. 12th International Conference on*, IEEE, 2009, pp. 363–372.
- [32] Chen, H., Chang, K., and Agate, C. S., “UAV path planning with tangent-plus-Lyapunov vector field guidance and obstacle avoidance,” *IEEE Transactions on Aerospace and Electronic Systems*, Vol. 49, No. 2, 2013, pp. 840–856.
- [33] Liang, Y. and Jia, Y., “Tangent vector field approach for curved path following with input saturation,” *Systems & Control Letters*, Vol. 104, June 2017, pp. 49–58.
- [34] Pereira, G. A. S., Choudhury, S., and Scherer, S., “A framework for optimal repairing of vector field-based motion plans,” IEEE, June 2016, pp. 261–266.
- [35] Pimenta, L. C., Pereira, G. A., and Mesquita, R. C., “Fully continuous vector fields for mobile robot navigation on sequences of discrete triangular regions,” *Robotics and Automation, 2007 IEEE International Conference on*, IEEE, 2007, pp. 1992–1997.
- [36] Md, Z., Rg, C., and Dj, G., “Simplex Solutions for Optimal Control Flight Paths in Urban Environments,” *Journal of Aeronautics & Aerospace Engineering*, Vol. 06, No. 03, 2017.
- [37] Zhou, D. and Schwager, M., “Vector field following for quadrotors using differential flatness,” IEEE, May 2014, pp. 6567–6572.
- [38] Goncalves, V. M., Pimenta, L. C. A., Maia, C. A., and Pereira, G. A. S., “Artificial vector fields for robot convergence and circulation of time-varying curves in n-dimensional spaces,” IEEE, 2009, pp. 2012–2017.
- [39] Goncalves, V. M., Pimenta, L. C., Maia, C. A., Pereira, G. A., Dutra, B. C., Michael, N., Fink, J., and Kumar, V., “Circulation of curves using vector fields: actual robot experiments in 2D and 3D workspaces,” *Robotics and Automation (ICRA), 2010 IEEE International Conference on*, IEEE, 2010, pp. 1136–1141.

- [40] Goncalves, V. M., Pimenta, L. C., Maia, C. A., Dutra, B. C., and Pereira, G. A., “Vector fields for robot navigation along time-varying curves in n -dimensions,” *IEEE Transactions on Robotics*, Vol. 26, No. 4, 2010, pp. 647–659.
- [41] Gerlach, A. R., *Autonomous Path-Following by Approximate Inverse Dynamics and Vector Field Prediction*, University of Cincinnati, 2014.
- [42] Ren, W., McLain, T., Sun, J.-S., and Beard, R., “Experimental validation of an autonomous control system on a mobile robot platform,” *IET Control Theory & Applications*, Vol. 1, No. 6, Nov. 2007, pp. 1621–1629.
- [43] Louali, R., Djouadi, M. S., Nemra, A., Bouaziz, S., and Elouardi, A., “Designing embedded systems for fixed-wing UAVs: Dynamic models study for the choice of an emulation vehicle,” IEEE, Feb. 2014, pp. 1–6.
- [44] Louali, R., Elouardi, A., Bouaziz, S., and Djouadi, M. S., “Experimental Approach for Evaluating an UAV COTS-Based Embedded Sensors System,” *Journal of Intelligent & Robotic Systems*, Vol. 83, No. 2, Aug. 2016, pp. 289–313.
- [45] Kapitanyuk, Y. A., Proskurnikov, A. V., and Cao, M., “A Guiding Vector-Field Algorithm for Path-Following Control of Nonholonomic Mobile Robots,” *IEEE Transactions on Control Systems Technology*, 2017, pp. 1–14.
- [46] Schmitt, S., Le Bars, F., Jaulin, L., and Latzel, T., “Obstacle Avoidance for an Autonomous Marine RobotA Vector Field Approach,” *Quantitative Monitoring of the Underwater Environment*, Springer, 2016, pp. 119–131.